To be published in Proceedings
of the 1969 Quantum Electronics
Conference, Chania, Greece
(Gordon and Breach, publishers)

RECEIVED
LAWRENCE
RADIATION LABORATORY

UCRL-20541
Preprint

c.2

DOCUMENTS SECTION

EFFECTS ON THE PROPAGATION OF OPTICAL BEAMS DUE TO SELF-INDUCED CHANGES IN INDEX OF REFRACTION

R. A. Fisher, J-P. E. Taran, R. Y. Chiao,
T. K. Gustafson and P. L. Kelley

March 1971

AEC Contract No. W-7405-eng-48

TWO-WEEK LOAN COPY

This is a Library Circulating Copy which may be borrowed for two weeks. For a personal retention copy, call Tech. Info. Division, Ext. 5545

LAWRENCE RADIATION LABORATORY
UNIVERSITY of CALIFORNIA BERKELEY

UCRL-20541 c.2

DISCLAIMER

This document was prepared as an account of work sponsored by the United States Government. While this document is believed to contain correct information, neither the United States Government nor any agency thereof, nor the Regents of the University of California, nor any of their employees, makes any warranty, express or implied, or assumes any legal responsibility for the accuracy, completeness, or usefulness of any information, apparatus, product, or process disclosed, or represents that its use would not infringe privately owned rights. Reference herein to any specific commercial product, process, or service by its trade name, trademark, manufacturer, or otherwise, does not necessarily constitute or imply its endorsement, recommendation, or favoring by the United States Government or any agency thereof, or the Regents of the University of California. The views and opinions of authors expressed herein do not necessarily state or reflect those of the United States Government or any agency thereof or the Regents of the University of California.

Effects on the Propagation of Optical Beams Due to Self-Induced Changes in Index of Refraction

R.A. Fisher*,**J-P.E. Taran†, R.Y. Chiao‡
Department of Physics, University of California
Berkeley, California 94720

T.K. Gustafson §
Department of Electrical Engineering and Computer Sciences,
Electronics Research Laboratory, University of California
Berkeley, California 94720

P.L. Kelley ‖
Lincoln Laboratory, Massachusetts Institute of Technology
Lexington, Massachusetts 02173

---

*Work supported by both the National Science Foundation and the U.S. Atomic Energy Commission.

**Also with Inorganic Materials Research Div., Lawrence Radiation Lab.

† On leave of absence until September 1969 from Département d'Optique, Office National d'Etudes et de Recherches Aérospatiales, France (ONERA). Work supported in part by the U.S. Army, ONERA and Délégation Générale à la Recherche Scientifique et Technique, France.

‡ Alfred P. Sloan Fellow, partially supported by NASA.

§ Supported by both the National Science Foundation and the Joint Services Electronics Program.

‖ This work was sponsored by the Advanced Research Projects Agency of the Department of Defense.

I. Introduction

We describe some of the processes which occur when light beams pass through material systems which possess an intensity dependent refractive index. These effects include: self-trapping and self-focusing, intensity-dependent birefringence, four-photon scattering, and inelastic light scattering (taking into account the finite relaxation time of the induced index change), as well as self-induced distortion of the amplitude and phase of intensity-modulated plane waves (with consequent spreading in the frequency spectrum of the light). Since the bandwidth or the optical pulse may be substantially increased due to the self-phase-modulation process there is the possibility of obtaining subpicosecond pulses.

Such intensity-dependent phenomena can arise from the optical Kerr effect. Neglecting relaxation effects, this directly produces a nonlinear change in the optical refractive index which is proportional to the intensity of the optical beam. Most of the effects listed above have been observed experimentally for the optical Kerr effect. A simple model of the optical Kerr effect is obtained by considering the orientation of anisotropically polarizable molecules.

Another source of an intensity dependent refractive index is the two step process involving optical rectification and its inverse, the linear electro-optic effect. The influence upon the propagation and scattering is more complex since the difference frequency fields cause a propagating change in the optical refractive index.

II. Stimulated Scattering Arising from the Orientational Kerr Effect

We discuss stimulated light scattering for the case where the material mechanism involves the orientational Kerr effect. The orientational optical Kerr effect arises from alignment produced by the interaction of the electric field with the induced dipole moment of a molecule. The effect is particularly large in liquids composed of anistropic molecules (such as CS_2 or Nitrobenzene). In an electric field $\vec{E}$, a single molecule is subject to a torque $\vec{T} = \vec{E} \times \vec{P} = \vec{E} \times (\overleftrightarrow{\alpha} \cdot \vec{E})$, where $\vec{P}$ is the induced dipole moment and $\overleftrightarrow{\alpha}$ is the polarizability tensor. The torque is zero when the electric field is parallel to a symmetry axis of the molecule, and the equilibrium is stable when the electric field is along the axis of highest polarizability tends to orient along the electric field.

In finding an equation of motion, one neglects nonviscous molecular interactions except for the local field correction due to the <u>linear</u> dielectric constant. (More complicated intermolecular interactions can produce an intensity-dependent index in liquids of nominally isotropic molecules.) The equation for the average induced change in the susceptibility $\Delta\chi$ to second order in the field is given for axially symmetric molecules (CS_2, nitrobenzene) by[2,3]

$$\frac{d(\Delta\chi)}{dt} = -\frac{\Delta\chi}{\tau} + K E^2 \tag{2.1}$$

where $K\tau = \chi^{(3)} = \frac{\varepsilon_2}{4\pi} = \frac{n_2 n_o}{2\pi} = \frac{2}{45} \frac{(\alpha_{\parallel} - \alpha_{\perp})^2}{kT} N$ and

where τ is the relaxation time associated with the randomiza-

tion of the molecular orientation after the field is shut off suddenly. $\chi^{(3)}$ is the third order nonlinear susceptibility, ϵ_2 and n_2 are associated with the quadratic contribution to the dielectric constant and index of refraction, respectively. $\alpha_{\parallel}$ and $\alpha_{\perp}$ are the polarizability components parallel and perpendicular to the symmetry axis, N is the number of molecules per unit volume, k is Boltzman's constant and T is the temperature. In the idealization of spherical molecules, the relaxation time τ is approximately given by $\eta V/(kT)$ where η is the viscosity and V is the molecular volume. If we allow two fields $E_o = \frac{1}{2}\,\mathcal{E}_o e^{-i(\omega_o t - \vec{k}_o\cdot\vec{r})} + c.c.$ and $E = \frac{1}{2}\,\mathcal{E}' e^{-i(\omega' t - \vec{k}'\cdot\vec{r})} + c.c.$ and $\mathcal{E}_o \gg \mathcal{E}'$ both polarized in the same direction to interact, we get as a solution to (2.1)

$$\Delta\chi = \frac{K\tau}{2}\left(\frac{|\mathcal{E}_o|^2}{2} + \frac{\mathcal{E}_o^*\mathcal{E}' e^{-i(\vec{q}\cdot\vec{r} - \Omega t)}}{1 + i\Omega\tau} + c.c.\right) \qquad (2.2)$$

where $\vec{q} = \vec{k}' - \vec{k}_o$ and $\Omega = \omega' - \omega_o$.

This susceptibility modulates the incident laser wave and scattered waves to produce a polarization:

$$P = \Delta\chi E = \frac{K\tau}{4}\left[|\mathcal{E}_o|^2 (E_o + E') + \frac{|\mathcal{E}_o|^2}{1+i\Omega\tau}\,\mathcal{E}' e^{-i(\omega_o t - \vec{k}_o\cdot\vec{r})}\right.$$

$$\left. + \frac{\mathcal{E}_o^{*2}\mathcal{E}' e^{-i[(2\vec{k}_o - \vec{k}')\cdot\vec{r} - (2\omega_o - \omega')t]}}{1+i\Omega\tau} + c.c.\right] \qquad (2.3)$$

where $E = E_o + E'$.

Let us concentrate on the second term in the right-hand side of (2.3). This term can react back on the waves E′. The power transferred/unit volume is:

$$\mathcal{P}' = \overline{E' \frac{dP'}{dt}} = \mathrm{Re}\ \frac{K\tau}{4} |\mathcal{E}_o|^2 |\mathcal{E}'|^2 \frac{i\omega'}{1 + i\Omega\tau}$$

$$= \frac{1}{45} \frac{(\alpha_{\parallel} - \alpha_{\perp})^2}{2kT} N |\mathcal{E}_o|^2 |\mathcal{E}'|^2 \frac{\omega'\Omega\tau}{1 + \Omega^2\tau^2}$$

$$= \frac{d}{dt} \frac{\epsilon_o |\mathcal{E}'|^2}{8\pi} = \frac{\epsilon_o}{\tau_g} \frac{|\mathcal{E}'|^2}{8\pi} \qquad (2.4)$$

Hence, the gain per unit length is:

$$g = \frac{n_o}{c\tau_g} = \frac{1}{\ell_g} = \frac{4\pi}{c} \frac{(\alpha_{\parallel} - \alpha_{\perp})^2}{45kTn_o} N |\mathcal{E}_o|^2 \frac{\omega'\Omega\tau}{1 + \Omega^2\tau^2} \qquad (2.5)$$

Note that we have neglected the last term of (2.3) which corresponds to anti-Stokes generation and is important only in the near-forward directions. The gain (Fig. 2.1(a)) is positive for $\Omega > 0$ (i.e. for Stokes or down-shifted frequencies from the laser) and is negative for $\Omega < 0$ (i.e. for anti-Stokes or up-shifted frequencies there is absorption). This is a general property of stimulated light scattering and reflects the fact that Stokes shifts are associated with phonon production, leading to positive feedback, whereas anti-Stokes shifts are associated with phonon destruction, leading to negative feedback. The crossover point at $\Omega = 0$, therefore, naturally has zero gain. Another way of stating this is that as $\Omega \to 0$, the "phonon" rate of buildup decreases proportionately. Also intuitively obvious is that as $\Omega \gg 1/\tau$, the molecules are being driven so fast that

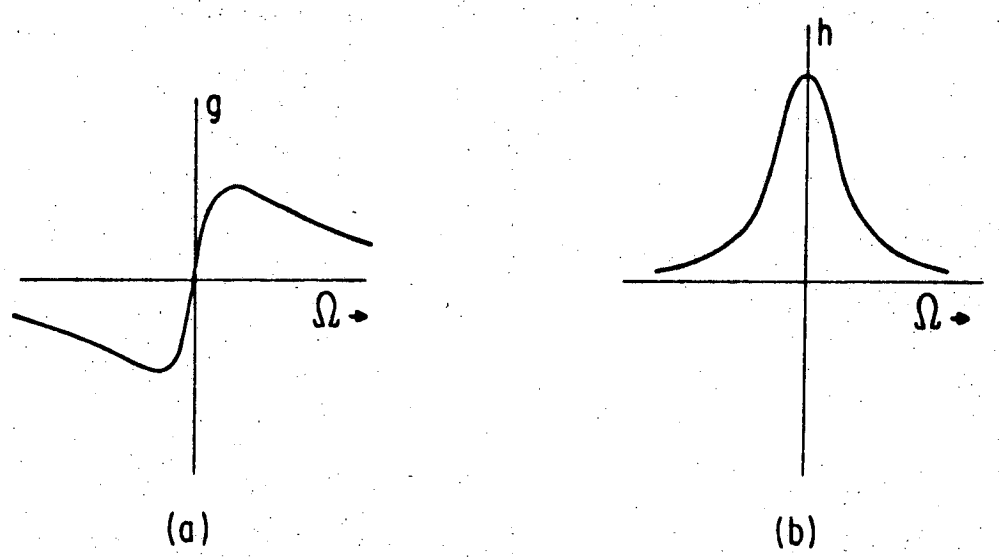

Fig. 2.1 a) Stimulated gain from Eq. 2.5. b) Spontaneous extinction coefficient.

they cannot respond and, hence, cannot react back on the field to produce much gain and, therefore, we expect that $g \to 0$ as $\Omega \to \infty$. The gain reaches a maximum between these two extremes at $\Omega = 1/\tau$ and one expects to observe gain narrowing to produce a sharp line at precisely $\Omega = 1/\tau$. This is in sharp contrast to the spontaneous scattering spectrum sketched in Fig. 2.1 (b), which is centered at $\Omega = 0$ and has Lorentzian wings. These wings are produced by kT-driven anisotropy fluctuations which decay with a time, τ, thus modulating and scattering the laser beam into a Lorentzian distribution.

Let us return to the formula for the induced polarization given by (2.3) and set $\Omega = 0$ and add an anti-Stokes wave[4] E'' given by

$$E'' = \tfrac{1}{2}\mathcal{E}'' e^{i(\vec{k}''\cdot\vec{r} - \omega'' t)} + c.c. \tag{2.6}$$

where $\vec{k}'' = 2\vec{k}_o - \vec{k}'$ and $\omega'' = 2\omega_o - \omega' = \omega_o$

in this case, when $\Omega = 0$. Then (2.3) becomes

$$P = \frac{K\tau}{4}\Big[|\mathcal{E}_o|^2 (E_o + 2E' + 2E'') + \mathcal{E}_o^{*2}\, \mathcal{E}' e^{-i(\vec{k}''\cdot\vec{r} - \omega'' t)}$$

$$+ \mathcal{E}_o^{2}\, \mathcal{E}''^{*} e^{i(\vec{k}'\cdot\vec{r} - \omega' t)} + c.c.\Big] \tag{2.7}$$

Note the factor of 2 in front of E' and E''. This represents the phenomenon of "weak-wave-retardation". This phenomenon arises whenever a strong and a weak wave interact in a nonlinear material, and manifests itself as an extra slowing down of the weak wave over and above that of the strong wave. From (2.7) the strong wave is slowed down by:

$$\Delta\chi_{strong} = \chi^{(3)} \frac{|\mathcal{E}_o|^2}{2} \text{ or } \Delta n_{strong} = \frac{\pi\chi^{(3)}}{n_o}|\mathcal{E}_o|^2 = n_2\frac{|\mathcal{E}_o|^2}{2} \qquad (2.8)$$

The weak wave is slowed down by twice this amount:

$$\Delta\chi_{weak} = \chi^{(3)} |\mathcal{E}_o|^2 \text{ or } \Delta n_{weak} = n_2 |\mathcal{E}_o|^2 \qquad (2.9)$$

Thus, the relative index change, which lengthens $|\vec{k}'|$ and $|\vec{k}''|$ is:

$$\Delta n = \Delta n_{weak} - \Delta n_{strong} = \pi\chi^{(3)}\frac{|\mathcal{E}_o|^2}{n_o} = \epsilon_2 \frac{|\mathcal{E}_o|^2}{4n_o} = \frac{n_2|\mathcal{E}_o|^2}{2} \qquad (2.10)$$

Physically, this retardation exists because in addition to the overall index change produced by the strong field, there exists a coherent phast-grating arising from the beating of the strong and weak waves. This Bragg grating reflects the strong wave into the weak wave direction, inducing an in-phase polarization. Since this polarization is in phase with E′, it slows E′ down through an index change $\Delta n = n_2|\mathcal{E}_o|^2/2$ as indicated in Fig. 2.2(a). The converse process of reflecting the weak wave into the strong wave direction is negligible ($\mathcal{E}_o \gg \mathcal{E}', \mathcal{E}''$) and thus the strong is not slowed down any amount comparable to Δn. Note that the Bragg grating is shown at 45° for simplicity.

This phenomenon implies that even in the absence of dispersion, the weak waves E′ and E″ interact most strongly at a <u>non-zero</u> angle θ_{opt}, sketched in Fig. 2.2(b) where $\Delta k = \Delta n \frac{\omega_o}{c}$. Hence, $k'\cos\theta_{opt} = k_o$ so for small θ_{opt}, $(1 - \frac{\theta_{opt}^2}{2})k' = k_o$ or $k'\frac{\theta_{opt}^2}{2} = \Delta k$ from which we get:

$$\theta_{opt} = \left(\frac{2\Delta k}{k_o}\right)^{\frac{1}{2}} = \left(\frac{2\Delta n}{n_o}\right)^{\frac{1}{2}} = \left(\frac{\epsilon_2|\mathcal{E}_o|^2}{2\epsilon_o}\right)^{\frac{1}{2}} = \left(\frac{n_2|\mathcal{E}_o|^2}{n_o}\right)^{\frac{1}{2}} \qquad (2.11)$$

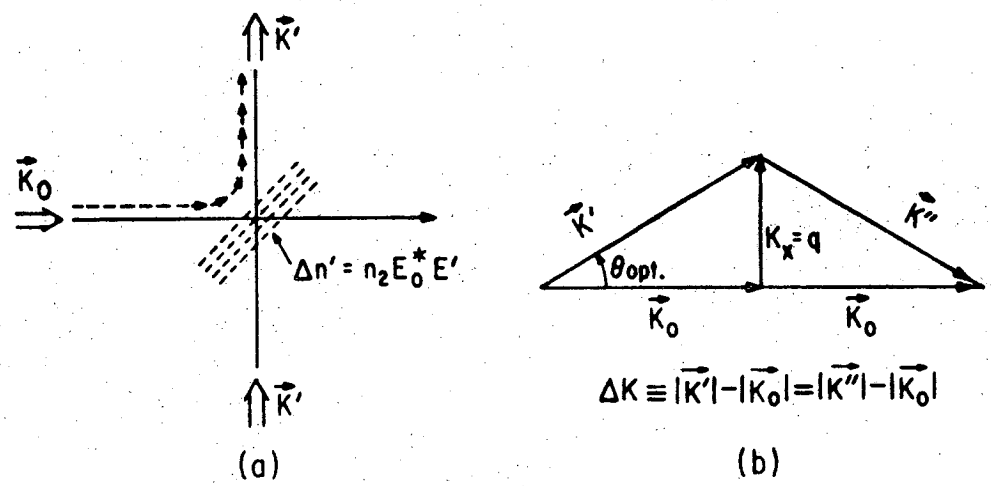

Fig. 2.2 a) Diagram of weak-wave retardation. b) Four-photon parametric process.

At this angle the weak-waves react back on each other so as to transfer power by amounts:

$$\mathcal{P}' = -\overline{E'' \frac{d\Delta P''}{dt}} = \omega_o \frac{\chi^{(3)}}{4} \operatorname{Im} (\mathcal{E}_o^2 \mathcal{E}'^* \mathcal{E}''^*) \tag{2.12}$$

$$\mathcal{P} = -\overline{E' \frac{d\Delta P'}{dt}} = \omega_o \frac{\chi^{(3)}}{4} \operatorname{Im} (\mathcal{E}_o^2 \mathcal{E}'^* \mathcal{E}''^*) \tag{2.13}$$

Equations (2.12) and (2.13) show that if ϕ_o, ϕ', and ϕ'' are the phases of $\mathcal{E}_o$, $\mathcal{E}'$, and $\mathcal{E}''$ respectively, choosing $2\phi_o - \phi' - \phi'' = \pi/2$, we automatically insure the simultaneous buildup of both weak waves at the expense of the strong wave $\vec{E}_o$. One can state this process quantum mechanically as follows: two incident laser photons scatter off each other and produce photons in $\vec{k}'$ and $\vec{k}''$ directions. This process is sometimes called light-by-light scattering or four-photon parametric amplification. To calculate the simultaneous gain, we set:

$$\begin{aligned} \omega_o \frac{\chi^{(3)}}{4} |\mathcal{E}_o|^2 \; |\mathcal{E}'| \; |\mathcal{E}''| &= \frac{\epsilon_o}{\tau_g} \frac{|\mathcal{E}'|^2}{8\pi} \\ \omega_o \frac{\chi^{(3)}}{4} |\mathcal{E}_o|^2 \; |\mathcal{E}'| \; |\mathcal{E}''| &= \frac{\epsilon_o}{\tau_g} \frac{|\mathcal{E}''|^2}{8\pi} \end{aligned} \tag{2.14}$$

So by multiplying together we get:

$$g = \frac{n_o}{c\tau_g} = \frac{2\pi}{n_o c} \omega_o \chi^{(3)} |\mathcal{E}_o|^2 = \frac{n_2 |\mathcal{E}_o|^2}{n_o} k_o = \theta_{opt}^2 k_o \tag{2.15}$$

This gain is twice the maximum gain of the anistropy-fluctuation scattering at $\Omega = 1/\tau$. For example, CS_2 (a Kerr liquid with $\epsilon_2 = 7.5 \times 10^{-11}$ esu) has a gain of about $10^{-2}\,cm^{-1}\,(Mw/cm^2)$, for the light-by-light process and half this amount for

anisotropy-fluctuation scattering. These values are comparable to the stimulated Raman and Brillouin gains. However, since light-by-light scattering involves no shift in frequency, it does not suppress the gain for other processes by laser depletion. In fact, since this effect will produce self-focussing, it enhances the other gains. A typical value of θ_{opt} given for CS_2 is 2.8×10^{-4} rad per (M watt/cm^2)$^{\frac{1}{2}}$. A more general treatment which includes both light-by-light and stimulated anisotropy-fluctuation scattering starts with letting three waves $E = E_o + E' + E''$ ($E', E'' \ll E_o$) interact in the medium. As usual we let:

$$E_o = \tfrac{1}{2}\mathcal{E}_o e^{i(\vec{k}_o \cdot \vec{r} - \omega_o t)} + c.c.,$$

$$E' = \tfrac{1}{2}\mathcal{E}' e^{i(\vec{k}' \cdot \vec{r} - \omega' t)} + c.c., \qquad (2.16)$$

$$E'' = \tfrac{1}{2}\mathcal{E}'' e^{i(\vec{k}'' \cdot \vec{r} - \omega'' t)} + c.c.$$

where, however, we make the slightly different choice for our k's:

$$k_o^2 - \frac{\omega_o^2 \epsilon_o}{c^2} - 4\pi \frac{\chi^{(3)}}{2c^2} |\mathcal{E}_o|^2 \omega_o^2 = 0,$$

$$(2.17)$$

$$k'^2 - \frac{\omega'^2 \epsilon_o}{c^2} - 4\pi \frac{\chi^{(3)}}{2c^2} |\mathcal{E}_o|^2 \omega'^2 = 0.$$

For simplicity we will neglect the frequency dispersion of the linear dielectric constant. We also write a similar equation for k''. This is in order to subtract out the strong-wave retardation common to all three waves. If we had made an error in

this choice, we can always correct it by taking $\mathcal{E}'$ and $\mathcal{E}''$ to be $e^{i\Delta kz}$ which is slowly varying. These waves produce a change in susceptibility:

$$\Delta\chi = \frac{\chi^{(3)}}{2}\left\{|\mathcal{E}_o|^2 + \frac{\mathcal{E}_o^* \mathcal{E}'}{1 + i\Omega\tau} e^{-i(\vec{q}\cdot\vec{r} - \Omega t)} + \frac{\mathcal{E}_o \mathcal{E}''^*}{1 + i\Omega\tau} e^{-i(\vec{q}\cdot\vec{r} - \Omega t)} + \text{c.c.}\right\} \tag{2.18}$$

Where as usual $\Omega = \omega_o - \omega' = \omega'' - \omega_o$ and $\vec{q} = \vec{k}_o - \vec{k}' = \vec{k}'' - \vec{k}_o$. Substituting the resulting nonlinear polarization into Maxwell's equation, we obtain:

$$-k_x^2 \mathcal{E}' + 2ik_z' \frac{\partial \mathcal{E}'}{\partial z} = -4\pi \frac{\chi^{(3)}}{2c^2} \omega'^2 \left\{|\mathcal{E}_o|^2 \mathcal{E}' + \mathcal{E}_o^2 \mathcal{E}''^*\right\} \frac{1}{1 + i\Omega\tau}$$

$$-k_x^2 \mathcal{E}''^* - 2ik_z'' \frac{\partial \mathcal{E}''^*}{\partial z} = -4\pi \frac{\chi^{(3)}}{2c^2} \omega''^2 \left\{|\mathcal{E}_o|^2 \mathcal{E}''^* + \mathcal{E}_o^{*2} \mathcal{E}'\right\} \frac{1}{1 + i\Omega\tau} \tag{2.19}$$

where we assumed that $\mathcal{E}'$, $\mathcal{E}''$ are slowly varying functions of z, the direction of propagation of the strong wave. We allow for weak-wave retardation by allowing for a nonzero Δk (see Fig. 2.2(b)). Let us define $\theta = k_x/k_o$ as our independent variable (we expect maximum interaction to occur and, hence, maximum gain when $\theta = \theta_{opt}$, and this should come out of the calculation). Also, our ansatz for the behavior of $\mathcal{E}'$ and $\mathcal{E}''^*$ is

$$\begin{pmatrix} \mathcal{E}'(z) \\ \mathcal{E}''^*(z) \end{pmatrix} = \begin{pmatrix} \mathcal{E}'_o \\ \mathcal{E}''_o \end{pmatrix} e^{i\gamma z} \tag{2.20}$$

where γ is complex (the real part being the effect of retardation and the imaginary part being the gain). We shall also assume $k_z' \simeq k_z'' \simeq k_o$ and $\omega' \simeq \omega'' \simeq \omega_o$ since the scattering is almost elastic and no difference terms appear in the coupled equations. Hence, we get from putting the ansatz into the coupled equations,

$$\left(-\theta^2 - 2\frac{\gamma}{k_o}\right)\mathcal{E}' = -4\pi\frac{\chi^{(3)}}{2}\frac{1}{\epsilon_o}\left\{|\mathcal{E}_o|^2\mathcal{E}' + \mathcal{E}_o^2\,\mathcal{E}''^*\right\}\frac{1}{1+i\Omega\tau}$$

$$\left(-\theta^2 + 2\frac{\gamma}{k_o}\right)\mathcal{E}'' = -4\pi\frac{\chi^{(3)}}{2}\frac{1}{\epsilon_o}\left\{|\mathcal{E}_o|^2\mathcal{E}''^* + \mathcal{E}_o^{*2}\,\mathcal{E}'\right\}\frac{1}{1+i\Omega\tau} \tag{2.21}$$

or multiplying together

$$\left(-\theta^2 - 2\frac{\gamma}{k_o} + 2\pi\frac{\chi^{(3)}}{\epsilon_o}\frac{|\mathcal{E}_o|^2}{1+i\Omega\tau}\right)\left(-\theta^2 + 2\frac{\gamma}{k_o} + 2\pi\frac{\chi^{(3)}}{\epsilon_o}\frac{|\mathcal{E}_o|^2}{1+i\Omega\tau}\right)$$

$$= \left(2\pi\frac{\chi^{(3)}}{\epsilon_o}\frac{|\mathcal{E}_o|^2}{1+i\Omega\tau}\right)^2 \tag{2.22}$$

or

$$\theta^4 - \frac{4\pi\chi^{(3)}}{\epsilon_o}\frac{|\mathcal{E}_o|^2}{1+i\Omega\tau}\theta^2 - 4\left(\frac{\gamma}{k_o}\right) = 0$$

Hence,

$$\gamma_\pm = \pm\frac{k_o}{2}\theta\left(\theta^2 - \frac{4\pi\chi^{(3)}}{\epsilon_o}\frac{|\mathcal{E}_o|^2}{1+i\Omega\tau}\right)^{\frac{1}{2}} = \pm\frac{k_o\theta}{2}\left(\theta^2 - \frac{2\theta_{opt}^2}{1+i\Omega\tau}\right)^{\frac{1}{2}} \tag{2.23}$$

The power gain $g = -2\,\mathrm{Im}\,\gamma_- = \frac{k_o\theta}{2}\left\{-a + (a^2+b^2)^{\frac{1}{2}}\right\}^{\frac{1}{2}}$ where

$a = \theta^2 - \dfrac{\theta^2_{opt}}{1 + \Omega^2\tau^2}$ and $b = 2\theta^2_{opt}\dfrac{\Omega\tau}{1 + \Omega^2\tau^2}$. This gain is sketched in Fig. 2.3.

The maximum gain occurs at θ_{opt} for $\Omega\tau = 0$ and as we noted previously, this gain corresponding to the degenerate ($\Omega = 0$) light-by-light process is twice that of the inelastic gain maximum ($\Omega\tau = 1$) for large angles

$$\gamma_- \simeq \frac{-k_o\theta^2}{2}\left(1 - \frac{\theta^2_{opt}}{\theta^2(1 + i\Omega\tau)}\right)$$

and

$$g(\text{large angles}) = -2\ \text{Im}\ \gamma_- = k_o\theta^2_{opt}\frac{\Omega\tau}{1 + \Omega^2\tau^2} \qquad (2.24)$$

which checks with our previous expression for stimulated anisotropy-fluctuation gain. This process is related to self-focussing and self-trapping in the following qualitative way: various spatial Fourier components of the beam scatter into components at larger angles and thereby decrease the beam diameter. For a Gaussian beam of diameter, d, we know that $k_{x\,max} = 2/d$ is the cutoff Fourier component. In the limit $|\mathcal{E}_o| \to \infty$, the gain at this component is $g \simeq \dfrac{k_o\theta_{max}}{2}\sqrt{2}\,\theta_{opt}$. If we set this equal to the inverse of some characteristic focussing length z_f, which clearly has the physical significance as the distance in which something has happened to diminish the beam diameter, then

$$z_f = \frac{d}{2}\left(\frac{\epsilon_2|\mathcal{E}_o|^2}{4\epsilon_o}\right)^{-\frac{1}{2}} = \frac{d}{2}\left(\frac{n_2|\mathcal{E}_o|^2}{2n_o}\right)^{-\frac{1}{2}} \qquad (2.25)$$

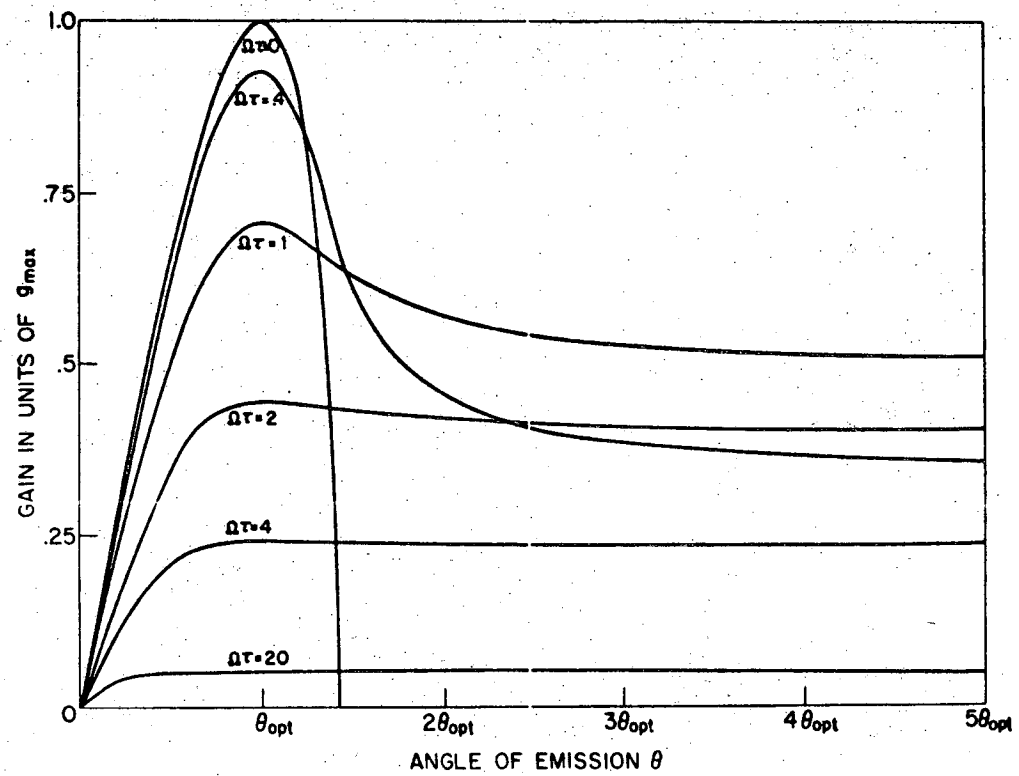

Fig. 2.3 Angular dependence of gain of stimulated Rayleigh-wing scattering.

In fact at this distance, the beam focusses down to a singularity,[5] as can be seem from the following reasoning: as a beam profile enters the liquid, it produces an index profile (since $\Delta n \propto$ intensity) which mimics the effect of a lens. This lens is convergent if $n_2 > 0$ and proceeds to produce a shorter focal length lens, etc. as indicated in Fig. 2.4 (a). This process leads to a singularity, as verified by machine calculation. This singularity is called the "self-focussing point" or "first-focus". This distance from the cell face, z_f, at which this occurs can be estimated from the following qualitative argument: consider what happens to the two rays (1 and 2) of Fig. 2.3.

The index differs by an amount $\Delta n = n_2 |\mathcal{E}_o|^2/2$ for rays 1 and 2 and produces a focus in a distance z_f from the initial boundary of the medium determined from Fermat's principle:

$$\int_{\text{path 1}} n \, dl = \int_{\text{path 2}} n \, dl \tag{2.26}$$

where we have assumed the initial phase fronts to be plane. Using the fact that $s \cong \sqrt{z_f^2 + (\frac{d}{2})^2} \cong z_f(1 + \frac{d^2}{8z_f^2})$, we obtain

$$(n_o + \Delta n)\, z_f = n_o s = n_o z_f \left(1 + \frac{d^2}{8z_f^2}\right) \tag{2.27}$$

or

$$z_f = \frac{d}{2}\left(\frac{n_o}{2\Delta n}\right)^{\frac{1}{2}} , \tag{2.28}$$

which differs from (2.25) by a factor of $\sqrt{2}$.

Self-trapping occurs when we distribute the Fourier components in such a way that these components light-by-light scatter self-consistently to reproduce the same distribution

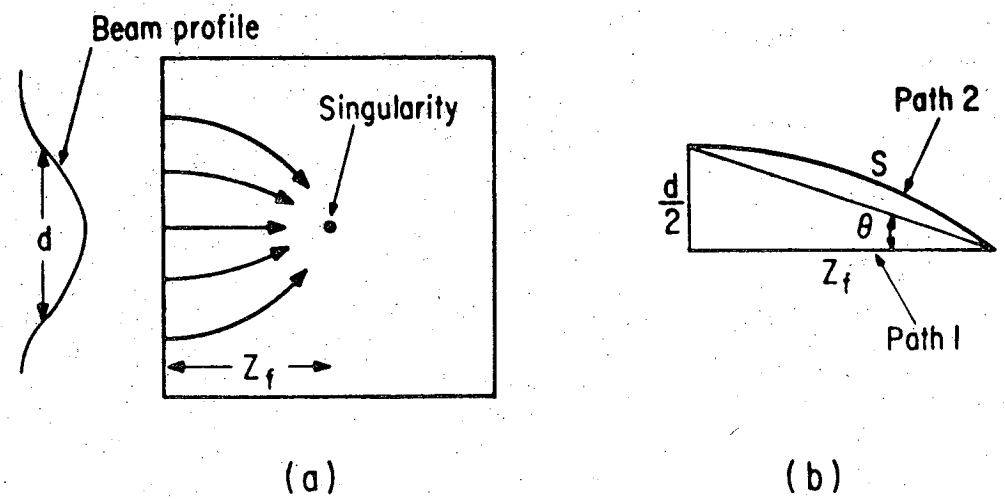

Fig. 2.4 a) Schematic of self-focusing. b) Simple model for calculating the self-focusing distance z_f.

of Fourier components except for a phase shift, which corresponds to an overall slowing down of a trapped intensity profile. Qualitatively, this occurs when $\theta_{opt} \simeq 1.22\ \lambda/d$ which leads to the correct self-trapping threshold. Another simple way to describe self-trapping is that the intensity-dependent index change causes a critical angle to develop

$$\cos\ \theta_{crit} = \frac{n_o}{n_o + \Delta n}$$

$$1 - \frac{\theta^2_{crit}}{2} = 1 - \frac{\Delta n}{n_o} \qquad (2.29)$$

or

$$\theta_{crit} = \left(\frac{2\Delta n}{n_o}\right)^{\frac{1}{2}} = \left(\frac{n_2 |\mathcal{E}_o|^2}{n_o}\right)^{\frac{1}{2}}$$

Notice that $\theta_{crit} = \theta_{opt}$ although physically they correspond to surface and volume phenomena respectively. Self-trapping occurs when the diffraction angle $\theta_{diff} = \frac{1.22\lambda}{n_o d} \simeq \theta_{crit}$. Thus, there exists a power threshold:

$$P = n_o \frac{c}{8\pi} |\mathcal{E}_o|^2 \pi d^2 = \frac{(1.22\lambda)^2 c}{128 n_2} \qquad (2.30)$$

Note that this is a power threshold, not an intensity threshold. This occurs because if one decreases the beam diameter to increase the beam intensity, one has a compensating effect of increased beam diffraction and the two effects balance. A machine calculation of the correct intensity profile which will propagate without change except for a phase change, yields a threshold very close to the value given by the above argument. Furthermore, the machine solution states that the phase change is of an amount

$$n_{eff} = \frac{k_z}{k_o} = \left(n_o^2 + \frac{\epsilon_2 |\mathcal{E}_o|^2}{9.72}\right)^{\frac{1}{2}} .$$

Associated with self-trapping are the phenomena of self-phase modulation and self-steepening, in which a pulse of light, due to the fact that its intensity and, hence, its index change varies with time, undergoes a modulation of its phase (i.e. frequency modulation) and a distortion of the intensity envelope (i.e. its peak travels slower than its skirts), eventually leading to a "shock" involving an infinite slope in the pulse shape. We will discuss the self-phase modulation in the next section.

III. Kerr Effect Self-Modulation

The propagation of optical pulses and other complex wave forms through media with an intensity-dependent index of refraction results in both a self-steepening of the envelope and a phase perturbation driven by the nonlinear dielectric change (which can be called self-phase modulation). These processes, particularly that of self-phase modulation, produce sidebands[7] which have been observed[8-10] in the frequency spectra of small-scale trapped filaments of laser light[11].

The characteristics of the light pulse propagation are based upon a traveling wave equation obtained from a Fourier analysis of the wave equation, using a general approach in which dispersion is easily included. If the electric field is specified by $E(z,t) = \frac{1}{2}\left(\mathcal{E}(z,t)e^{i(k_o z-\omega_o t)} + c.c.\right)$, k_o and ω_o being the carrier propagation vector and the frequency, one obtains the following complex propagation equation for the electric field envelope[12]

$$\left(\frac{c}{\sqrt{\epsilon_o}}\frac{\partial}{\partial z} + \frac{\partial}{\partial t}\right)\mathcal{E}(z,t) = \frac{1}{2}\left[i\omega_o - \frac{1}{2}\left(\frac{c}{\sqrt{\epsilon_o}}\frac{\partial}{\partial z} - \frac{3}{2}\frac{\partial}{\partial t}\right)\right]\left[\frac{\delta\epsilon}{\epsilon_o}\mathcal{E}(z,t)\right] \quad (3.1)$$

where $\delta\epsilon$ is the nonlinear change in the dielectric coefficient which is assumed to be much less than 1.

We concern ourselves with Kerr liquids, for which the non-linear change in displacement, δD, can be written in the form

$$\delta D(t) = \delta\epsilon(t)E(t) \quad (3.2)$$

where $\delta\epsilon(t)$ is the intensity-dependent part of the dielectric coefficient given by (2.1). Since $1/\tau$ is much less than optical frequencies, molecular orientation cannot respond to opti-

cal variations in the torque resulting from the applied electric field and the induced molecular dipole moment. Consequently, $\delta\epsilon$ effectively responds only to the part of E^2 which does not vary at optical frequencies. For CS_2 the value of ϵ_2 which is defined after (2.1) is about 7.5×10^{-11} esu.

The effects produced by the propagation of a pulse through the medium are investigated primarily through spectral analysis. The relevant power spectrum as observed is given by

$$S(Q,\Omega) = \frac{c}{8\pi} \operatorname{Re} \{ \mathcal{E}(Q,\Omega)\, \mathcal{H}^*(Q,\Omega) \} \simeq \frac{c}{8\pi} \sqrt{\epsilon_o}\, |\mathcal{E}(Q,\Omega)|^2 \quad (3.3)$$

in which $\mathcal{E}(Q,\Omega)$ is the Fourier transform of the envelope $\mathcal{E}(z,t)$.

$$\mathcal{E}(Q,\Omega) = \frac{1}{2\pi} \int_{-\infty}^{\infty} dz \int_{-\infty}^{\infty} dt\, \mathcal{E}(z,t) e^{i(Qz - \Omega t)} \quad (3.4)$$

For distances which are very short compared to the shock distance[13], the self-steepening of the envelope is not appreciable. In this case the spectral development is almost entirely determined by the phase distortion which obeys

$$\left(\frac{c}{\sqrt{\epsilon_o}} \frac{\partial}{\partial z} + \frac{\partial}{\partial t}\right) \delta\phi(z,t) = \frac{\omega_o}{2\epsilon_o}\, \delta\epsilon\, (z,t) \quad (3.5)$$

where $\delta\epsilon$ is found given as before by (2.1). The complex amplitude, $\mathcal{E}(z,t)$ has been expressed as $a(z,t)e^{-i\delta\phi(z,t)}$ where $a(z,t)$ and $\delta\phi(z,t)$ are real. If we assume a^2 to have a fixed shape for all z, and assuming $\delta\phi(z = o,t) = 0$, $\delta\phi$ becomes

$$\delta\phi(z,t) = \alpha \int_{-\infty}^{t} \frac{e^{-(t-t')/\tau}}{\tau} [a(z,t')/a_o]^2\, dt' \quad . \quad (3.6)$$

We define the phase parameter α to be $k_o z \epsilon_2 a_o^2/4\epsilon_o$, in which a_o^2 normalizes the initial intensity variation to unity.

The methods of stationary phase applied to Eq. (3.4) show that the frequency shift is approximately given by (minus) the time derivative of $\delta\phi$. Thus, the slope of the phase curve determines, to an important degree, the Fourier component associated with that part of the pulse. There are generally two points in the phase curve with the same slope and, as Shimizu[6] has pointed out, the corresponding contributions can interfere constructively or destructively depending on whether they differ in phase by an even or odd multiple of π. It can be shown that the maximum number of interference peaks is $\alpha/2\pi$. While the phase development is very significant we also must consider the shape of the envelope since the degree of interference will be determined in part by the amplitude ratio. Furthermore, the rate of change of slope of the phase will also influence the size of the contributions of each region.

The downshifted part of a filament spectrum is shown in Fig. 3.1. Curve (a) of this figure shows the theoretical self-modulation obtained by Cheung, et al[7] from Eq. (3.6), when $\tau = 0$. The optical wave envelope, $a^2(z,t)$ is assumed to possess a weak modulation at a frequency $\omega_s = 2.5\ cm^{-1}$. This envelope is independent of z since self-steepening was ignored. In comparison, curve (c) indicates the self-modulation obtained when $\tau = 0$, assuming a Gaussian envelope, $a^2(z,t)$, of full width 7.4 psec. Pulse distortion is taken into account but has little effect on the spectrum in this case since the distance is about 1/100 of the shock distance. The curves of both Figs. 3.1(a) and 3.1(c) fit the experimental spectrum (curve b)

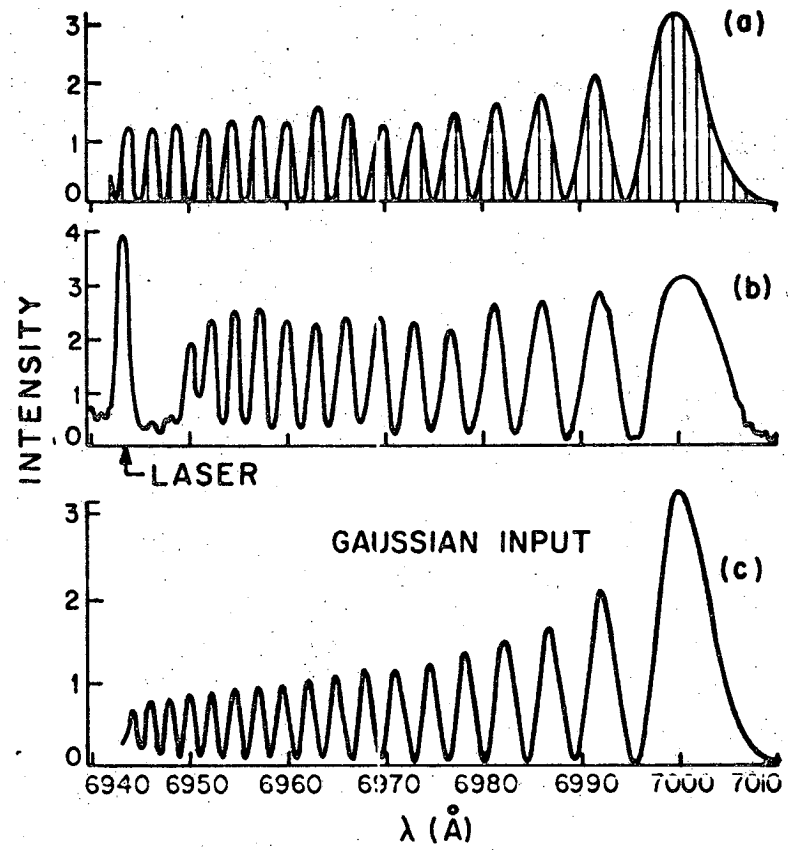

Fig. 3.1 Spectral broadening in CS_2. a) Theoretical calculation of Cheung et al.[7] b) Experimental spectrum of Cheung et al. c) Theoretical calculation assuming an initially Gaussian intensity profile. The full (1/e) width equals 7.4 psec and α = 107.

of Cheung et al[7] for CS_2.

It is evident that there is little difference between the overall spectral development for a single pulse and that for a sinusoidal modulation whose period is of the order of twice the width of the pulse. The spectrum for the sinusoid, however, does possess a discrete underlying structure whose components are spearated by ω_s, in contrast to the continuous spectrum for the pulse. A libration effect arising from an oscillation of the molecules about the electric field has been suggested[7] as a model giving rise to a sinusoidal modulation. Experimentally there are a few cases which show fine structure, possibly due to sinusoidal modulation.[11,14] There is apparently no fine structure associated with the largest frequency shifts contrary to what is expected for pure sinusoidal modulation. Variation in modulation frequency might blur out the discrete spectra in the region of large frequency shifts. The finite filament lifetime, if it is only a few modulation cycles, can also lead to a blurring of the fine structure.

If the spectra arise from pulses of the order of ten picoseconds, the origin is still uncertain. Spectra with the above characteristics have been observed in experiments using laser pulses at least as long as 100 psec. We, therefore, infer that pulses of this length, if present, are formed in the liquid. Nevertheless, the initial time structure of the laser is important since it plays a role in the nonlinear processes, including self-focusing.

The self-focusing process and stimulated scattering might give rise to trapped filaments whose temporal extent is of the order of one to ten picoseconds. Marburger and

Wagner[15] have pointed out that a pulse will become shortened in time as it travels from the cell entrance to the shortest self-focusing point in the beam. This process of chopping the wings of the pulse should continue until its width is the order of the relaxation time for orientation.[16] This process can also turn a smoothly modulated signal into a series of short pulses, which would have a spectrum exhibiting fine structure at the modulation frequency.

Stimulated scattering processes, for example Brillouin scattering in the backward (opposite to the laser beam) direction, could lead to a shortening of the self-trapped light pulse in a filament. This shortening would continue until the gain dropped to a low enough value to cut off the loss due to stinulated scattering. The Brillouin gain in this region will take on transient character.[17,18] The transient gain exponent can be given by

$$G = \sqrt{\frac{2g_o v_o}{\tau'}}\,\tau_p \quad . \tag{3.7}$$

Here g_o is the steady state gain per unit length, τ' is the phonon relaxation time, v_o is the velocity of light, and τ_p is the pulse length in time. Note that $g_o \propto \tau'$; therefore, G does not depend on τ'. In small scale filaments $g_o \approx 10^4 cm^{-1}$, $\tau' \approx 10^{-9}$ sec and assuming $G < 20$ for the instability to be ineffective, we find $\tau_p < 25$ psec.

From the above we conclude that pulse envelopes whose widths are of the order of the relaxation time or less in extent may result from the self-focusing process or from stimulated scattering processes occurring in the backward direction. In such cases the lagging edge of the phase, $\delta\phi(z,t)$, will possess an exponential tail with a decay time equal to the relaxa-

tion time, τ. Since this portion of the phase curve determines the upshifted Fourier components, we can immediately conclude that these components will be most affected by the relaxation. Figure 3.2 (a) shows a computer calculation of the pulse development at two distances including the effects of relaxation, while Fig. 3.2 (b) shows the phase development at the same distance (the initial phase was assumed to be zero). The relaxation time is taken to be 2 psec corresponding to CS_2.

The frequency spectrum corresponding to a propagation distance given by $\alpha = \alpha_1$ (Fig. 3.3) and illustrates the influence of relaxation, which is particularly noticeable on the anti-Stokes side. Of the two contributions from the envelope, a(z,t), to any upshifted Fourier component, the one nearest the envelope peak dominates more than in the case when $\tau \ll \tau_p$ since the other contribution will be out in the exponential tail of the phase curve where the envelope is smaller. Thus, the interference pattern shows less contrast for the upshifted part of the spectrum. However, as in the case when $\tau \ll \tau_p$, this interference effect increases with increasing upshift since the ratio of the two envelope amplitudes determining each frequency component tends to one.

In contrast, the entire Stokes spectrum exhibits a pronounced interference effect similar to that observed when $\tau \ll \tau_p$. We also notice that there is a compression of the frequency spectrum since the height of the phase curve is decreased due to the exponential tail.

We also see that the total intensity of the anti-Stokes components is less than that of the Stokes side due to the phase delay and the exponential tail.

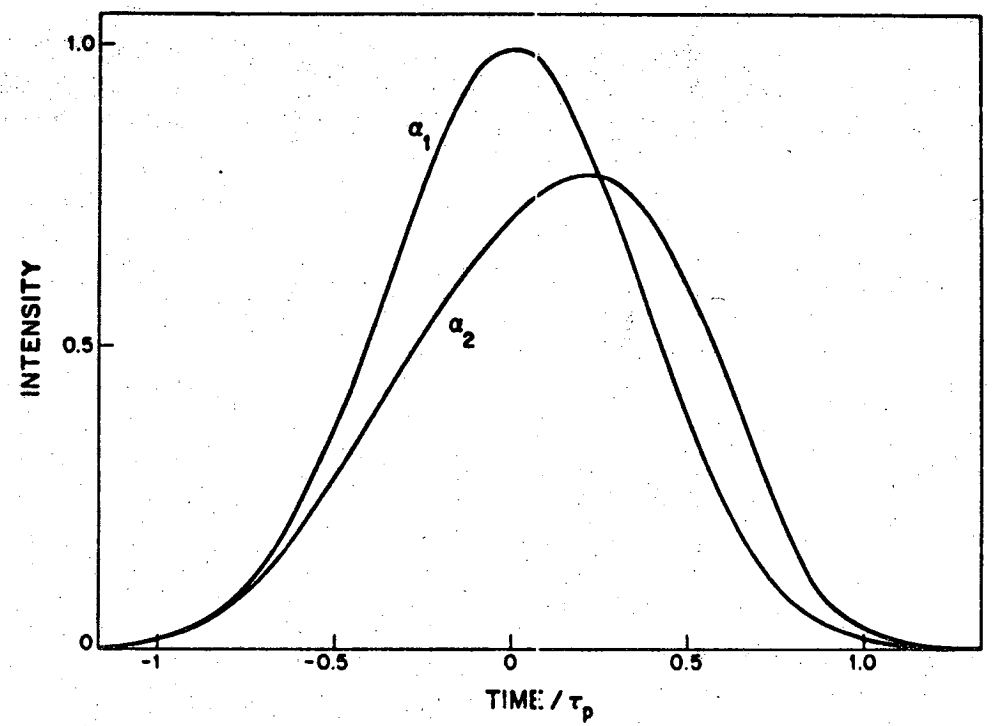

Fig. 3.2 Influence of relaxation upon the pulse development. The initial intensity is assumed Gaussian with full 1/e width, τ_p, given by $\omega_o\tau_p = 1.4 \times 10^4$ radians. The ratio of the relaxation to the pulse width, τ/τ_p, is .36. a) Intensity profiles normalized to the initial maximum intensity of the Gaussian plotted for two values of the phase parameter $\alpha_1 = 117$ and $\alpha_2 = 2396$. b) Corresponding phase curves, normalized with respect to α, assuming the initial phase to be zero.

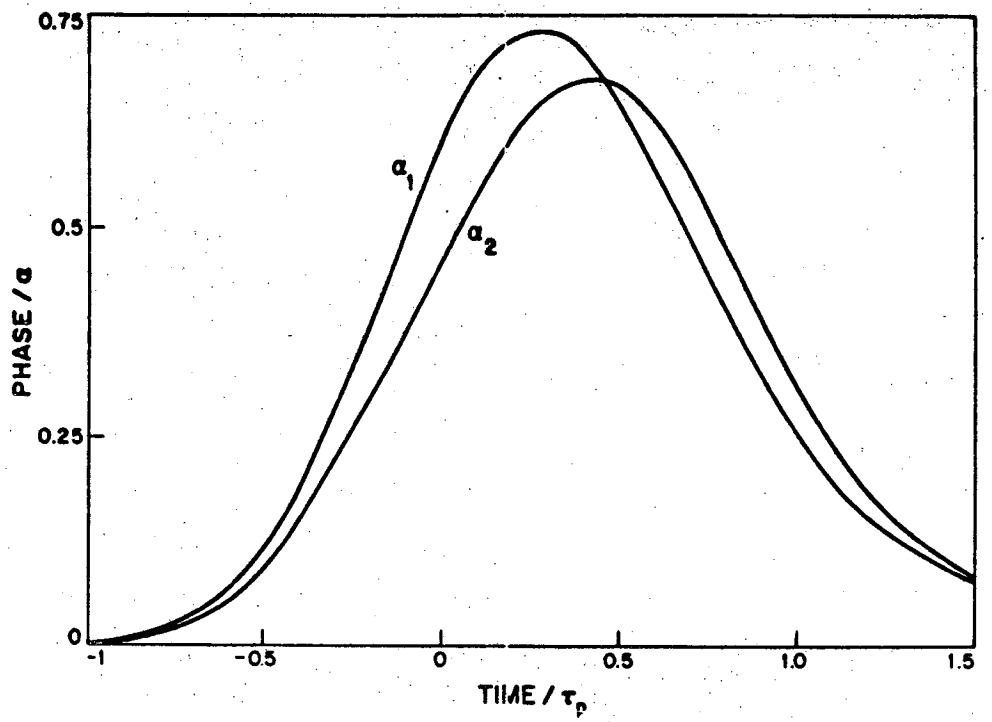

Fig. 3.3 Spectrum of the pulse of Fig. 3.2 for $\alpha = \alpha_1$ with ω_0 at the ruby frequency ($2\pi c/\omega_0 = 6943$ Å). τ_p is 5 psec and τ, the orientational relaxation time for CS_2, is 2 psec. The intensity is plotted in arbitrary units.

The relative importance of the above effects depends upon the detailed shape of the pulse and its length with respect to the relaxation time. However, many self-modulated filaments display the type of Stokes-anti-Stokes asymmetry illustrated in Fig. 3.3.[9, 11, 14]

Variation in observed spectra could be due to variation in pulse shape. A significant fraction of the filaments observed by various authors show weak upshifted wings which are more extensive than the intense downshifts. Such spectra might arise from pulses whose tails drop sharply. Stimulated scattering in the backward direction as well as self-steepening would produce a sharp tail. Noncollinear gain effects, not included in the present plane-wave calculation, will also have an effect on asymmetry. It has been shown that relaxation inhibits but does not prevent the steepening of the envelope[10] and the buildup of the phase. If lifetimes and propagation distances associated with the filaments are great enough, dispersion will ultimately become inportant, provided other spreading mechanisms are negligible.

Figure 3.4(a) shows an experimental spectrum taken with a mixture of two-thirds CS_2 and one-third benzene by volume. The spacing of the peaks close to the laser was about 3.5 cm^{-1}. A similar spectrum was obtained theoretically (Fig. 3.4b) using a Gaussian pulse of width 5.4 psec and a relaxation time of 9 psec. Perhaps the CS_2 orientational relaxation time is altered by the presence of the benzene. Deviation from Gaussian pulse shape might modify somewhat the parameters used.

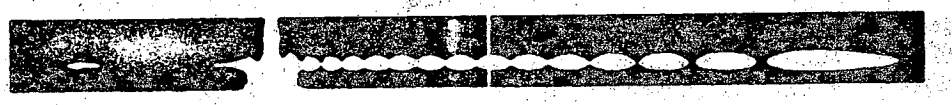

(a)

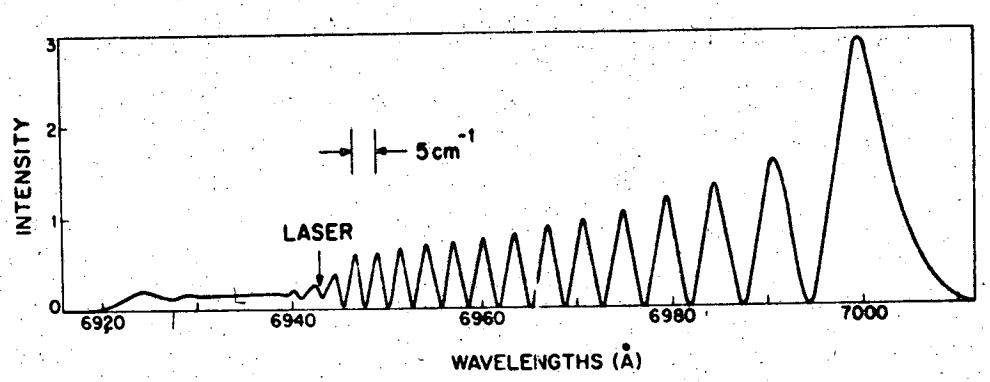

(b)

Fig. 3.4 Experimental spectrum and theoretical fit using a Gaussian pulse of width 5.4 psec, a relaxation time of 9 psec, and $\alpha = 265$.

IV. Electro-Optic Self-Phase Modulation

Optical retification and the electro-optic effect can combine to give self-phase modulation and pulse distortion. Optical rectification was first observed by Bass, et al[19] and difference frequency generation[20] as well as the production of millimeter waves by optical pulses have also been observed.[21] We will discuss the reaction back of the base-band (or rectified field) on the optical field. This phenomenon differs in a number of significant ways from Kerr effect self-modulation and envelope distortion. We show that a) an effective intensity-dependent refractive index change of either sign results, suggesting the presence of either or both self-focusing and defocusing, b) a novel spectrum of self-phase modulation is generated, c) non-linear pulse dispersion and self-steepening occur, d) new types of both stimulated and spontaneous light scattering and light-by-light scattering arise. All these new effects are a generalization of processes involved in parametric amplification and upconversion,[22] in that continuous sideband generation on both sides of the pump frequency occurs.

The simultaneous rectification and time-distortion of an optical pulse can be studied most simply for collinear propagation of the rectified and optical fields neglecting the radial profiles of both. For optical pulses longer than a few wavelengths the rectified field can be adequately described by a scalar wave equation. This is coupled to the optical field through the portion of the nonlinear polarization proportional to the optical field intensity so that

$$\left(\frac{\partial^2}{\partial z^2} - \frac{\epsilon_s}{c^2}\frac{\partial^2}{\partial t^2}\right) F = \tfrac{1}{2}\frac{4\pi\chi}{c^2}\frac{\partial^2}{\partial t^2}\mathcal{E}\mathcal{E}^* \quad . \tag{4.1}$$

Here χ is the effective value of the electro-optic coefficient appropriate for the particular direction of field polarization chose, ϵ_s is the effective static dielectric coefficient, and $\mathcal{E}$ the complex amplitude of the optical pulse as defined in section 3.

Through the electro-optic effect the induced field F produces a change in the dielectric coefficient of the medium which is given by $\delta\epsilon = 8\pi\chi F$. For intense short pulses, the resultant contribution to the polarization varying at the optical frequency can cause significant phase and amplitude distortions in the optical pulse. Such changes are goverened by the same approximate complex traveling wave equation for $\mathcal{E}$ employed for the Kerr effect modulation, Eq. (3.1). The imaginary term, on the right-hand side of (3.1) which provides the primary contribution, gives rise to a phase change across the pulse, whereas the remaining two terms effectively describe the influence of the nonlinearity upon the shape of the pulse envelope.

If the last two terms of (3.1) are neglected, only the phase of the optical pulse is affected by the rectified field which is generated. For this approximation, which is valid for short propagation distances and relatively small nonlinear changes, $\mathcal{E}\mathcal{E}^*$ is only a function of $\left(t - \frac{z}{v_o}\right)$, where $v_o = \frac{c}{\sqrt{\epsilon_o}}$ is the linear speed of the optical pulse. In this case the rectified field is excited by a phased array of distributed dipoles whose frequency spectrum is not varying with distance. The calculation of the field thus reduces to a problem of linear radiation theory. Choosing $z = 0$ at the input boundary of a crystal and assuming normal incidence of the waves, it can be

verified that the following solution satisfies (4.1)

$$F(t,z) = \frac{4\pi}{\epsilon_s - \epsilon_o} R_1' \; P\left(t + \frac{z}{v_s'}\right) \quad \text{for} \quad z < 0 \;,$$

$$= \frac{4\pi}{\epsilon_s - \epsilon_o} \left\{ -P\left(t - \frac{z}{v_o}\right) + T_1' \; P\left(t - \frac{z}{v_s'}\right) \right\} \text{for } z > 0, \tag{4.2}$$

with $v_s = \frac{c}{\sqrt{\epsilon_s}}$ and $v_s' = \frac{c}{\sqrt{\epsilon_s'}}$ and where $T_1' = \frac{\sqrt{\epsilon_o} + \sqrt{\epsilon_s'}}{\sqrt{\epsilon_s} + \sqrt{\epsilon_s'}}$ and

$R_1' = \frac{\sqrt{\epsilon_o} - \sqrt{\epsilon_s}}{\sqrt{\epsilon_s} + \sqrt{\epsilon_s'}}$.[23,24] ϵ_s and ϵ_s' are respectively the "static" dielectric constants inside and outside the crystal. We assume throughout that the crystal is antireflection coated at the optical frequency. Here, $P\left(t - \frac{z}{v_o}\right)$ is the dipole moment per unit volume, which for the electro-optic effect is

$$P\left(t - \frac{z}{v_o}\right) = \frac{\chi}{2} \left| \mathcal{E}\left(t - \frac{z}{v_o}\right) \right|^2 .$$

Many ferroelectric crystals, such as Barium Strontium Niobate (BSN) , have large linear electro-optic effects associated with extremely large static dielectric constants.[25,26] For these materials the rectified fields generated on the input surface and the bulk of the crystal are given directly by Eq. (4.2). Only the forced response to the driving nonlinear polarization travels with the optical pulse. For distances larger than $\frac{v_o^2 \tau_p}{v_o - v_s}$, the homogeneous response is delayed significantly. If ϵ_s is chosen to be equal to ϵ_s' , this portion of the rectified field crosses the boundary without reflection.

The resultant influence upon the optical pulse is very similar to that obtained from the Kerr effect but with a negative value for the Kerr coefficient. The phase change across the pulse after propagating through a crystal of length, L, is given by

$$\delta\phi = -\frac{-16\,\chi\pi^2}{\sqrt{\epsilon_o}(\epsilon_s-\epsilon_o)}\;\omega_o P(t-L/v_o)\,\frac{L}{c} + \Delta\phi \qquad (4.3)$$

where $\Delta\phi$ is the small contribution arising from the forward propagating homogeneous rectified pulse as well as reflections from the boundaries of the crystal. As before, for crystals appreciably larger than the pulse width this influences the phase only on the low intensity trailing portion of the intensity profile and consequently can be neglected. In contrast to the optical Kerr effect the leading edge of the optical pulse is frequency upshifted and the back edge is downshifted.[27] The power spectrum in the absence of dispersion is symmetrical and identical to that obtained for the orientational Kerr effect in the limit of a zero relaxation time.[6,7,9]

The most interesting situation arises when the optical pulse width $v_o\tau_p$ and the coherence length $v_o^2\tau_p/(v_o-v_s)$ are respectively much less and much greater than crystal length L. GaAs is an example of a material for which the coherence length will be of the order of centimeters. Both the homogeneous and driven rectified fields within the crystal then travel with the optical pulse and a resonant interaction occurs. By expanding the second term of (4.2) into a Taylor series about $(t - z/v_o)$, the singularity is eliminated and one obtains a finite field, a portion of which is linearly increasing in z.

$$F(t,z) = \frac{2\pi}{\sqrt{\epsilon_o}\,(\sqrt{\epsilon_o} + \sqrt{\epsilon'_s})}\, P(t + z/v'_s) \text{ for } z < 0$$

$$= \frac{-2\pi}{\sqrt{\epsilon_o}} \left\{ \frac{\partial P}{\partial t}\,(t - z/v_o)\,\frac{z}{c} + \frac{1}{\sqrt{\epsilon_o} + \sqrt{\epsilon'_s}} P(t-z/v_o) \right\} \text{for } z > 0. \tag{4.4}$$

This situation is analogous to the resonant excitation of a simple harmonic oscillator as is readily apparent for a purely sinusoidal intensity modulation.[24] The linearly increasing solution then displays the usual proportionality to frequency and 90° phase shift with respect to the modulation. In this context we note that the high frequency components combined with the high intensity of ultrashort pulses should greatly enhance the amount of rectification which can be achieved.

The fields subsequent to a reflection from the output boundary of the crystal are obtained by the usual continuity requirements.[28] When $\epsilon'_s = \epsilon_s$ the results are particularly simple. The portion of the field represented by the first term of (4.4) is transmitted while that represented by the third is reflected from the output boundary. In Fig. 4.1 (a) these general characteristics, which were obtained by solving (4.1) and (3.1) numerically, are illustrated for the case of propagation through an electro-optic material 12 mm in optical length, having $\epsilon_o = 5$ and an electro-optic coefficient of 2.0×10^{-8} esu. The initial pulse, which is assumed to be a Gaussian with a peak intensity of .25 gigawatts/cm^2 and a full $\frac{1}{e}$ width τ_p of 20 psec., displays little distortion and, at the time shown in Fig. 4.1 (a), would be centered on the right-hand rectified pulse. The pulse reflected from the output boundary

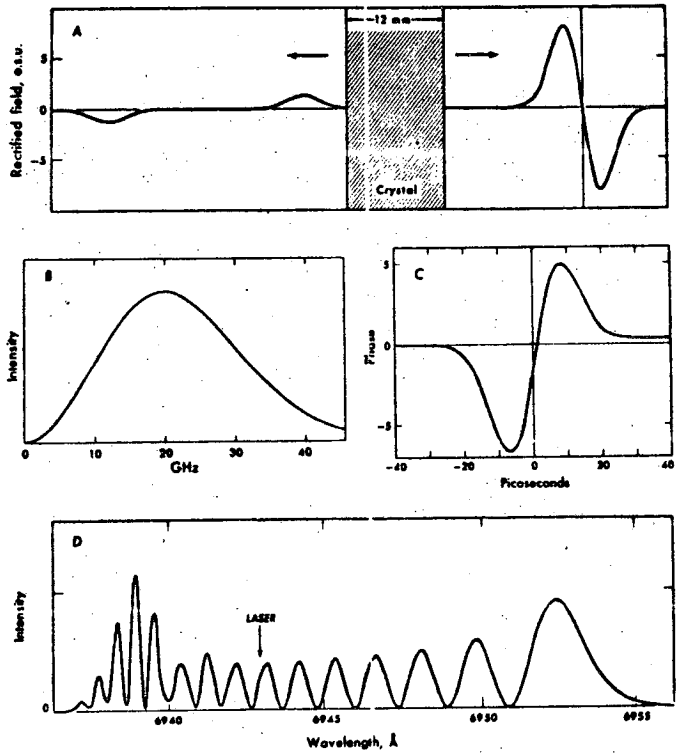

Fig. 4.1 Typical results in a crystal with $\epsilon_s = \epsilon_s' = \epsilon_o$. a) Snapshot of rectified fields at $t = 100$ psec after the optical pulse enters the crystal. The lengths are expressed in terms of optical thickness. The optical pulse has a Gaussian intensity profile of full 1/e width equal to 20 psec. Peak intensity is .25 Gw/cm^2. The electro-optic coefficient is chosen to be 2×10^{-8} e.s.u. b) Spectrum of the forward propagating rectified pulse shown in Fig. 4.1(a) c) Phase change across the optical pulse for the same conditions as above d) Spectrum of the self-phase modulated optical pulse for the same conditions as above, but with a crystal length of 24 mm.

has also propagated out of the crystal and lags the first pulse traveling in the backward direction by a distance of 2L. Since the forward propagating rectified pulse exhibits essentially one cycle of oscillation over the width of the optical pulse, its spectrum is broad with a peak at τ_p^{-1} (Fig. 4.1 (b)); this spectrum could be significantly narrowed by using mode-locked pulse trains in which successive pulses are separated by the pulse width. The two backward propagating pulses which are spearated by a distance of 2L, each possess the spectral shape of the optical intensity profile. Interference between the two pulses results in a shift of the peak of the spectrum from zero towards $(v_o/2L)$.

The phase change produced across the optical pulse by the rectified field of (4.4) is determined by integrating (3.1). Since we have assumed distortionless propagation, the last two terms of Eq. (3.1) are neglected and the electric field is of the form $\mathcal{E} = a\{(t-z/v_o)\}e^{i\delta\phi(t,z)}$ where the real amplitude, a, can be treated as a constant with respect to the integration. Using (4.4) in the expression for $\delta\phi$, one obtains

$$\delta\phi(z,t) = \frac{-4\omega_o\pi^2\chi}{\epsilon_o c}\frac{\partial P(t-z/v_o)}{\partial t}z^2 - \frac{2\omega_o\pi^2}{\epsilon_o c}\frac{P(t-z/v_o)}{(\sqrt{\epsilon_o}+\sqrt{\epsilon_s'})}z + \Delta\phi(z,t) \tag{4.5}$$

The third term arises from the portion of the rectified field which is reflected from the output boundary into the backward direction. For crystals which are longer than the pulse width, this only contributes in the low intensity region on the trailing edge of the optical pulse and hence is unimportant. It is this contribution which is responsible for the tail on the phase

curve of Fig. 4.1 (c), which begins to taper off at a time $2L/v_o$, the time at which the reflected rectified field begins crossing the input boundary.

The frequency shift for any portion of the optical pulse is given approximately by $-\frac{\partial}{\partial t}\delta\phi(z,t)$.[9, 10, 12] Assuming a crystal longer than the pulse width, the contribution quadratically increasing in z dominates. Consequently, the wings of the optical pulse are upshifted in frequency whereas the central portion exhibits a downshift. The resultant power spectrum, which is roughly proportional to $|\mathcal{E}(\Omega)|^2$ is shown in Fig. 4.1 (d) This is in contrast to the behavior of the Kerr effect for which a linear distance dependence is predicted [10,12] and experimentally verified.[29] The resultant Stokes spectra are quite similar; however, the anti-Stokes shift for the linear electro-optic effect contains additional interference which is not present for the quadratic Kerr effect. This originates from interference of the four localized portions of the pulse profile experiencing approximately the same frequency upshift. An overall interference pattern similar to that obtained from the Kerr effect is produced by the interference within either of the two upshifted regions whereas the superimposed fine structure arises from the cross-interference between these two regions . The separation between the interference maxima of this fine structured region is approximately the inverse of the optical pulse width. Experimentally, the presence of such a fine structure would be strong evidence for the presence of millimeter radiation generated by the rectification process.

For the intermediate case $\frac{v_o^2 \tau_p}{v_o - v_s}$ is of the order of the

crystal length; the homogeneous and forced responses to the polarization, then combine to produce a spectrum between that of Fig. 4.1 (d) and Fig. 3.1. However, for such a situation the homogeneous rectified fields partially reflected from the output boundary could also significantly alter the phase change, and hence the optical spectrum.

We have also investigated the propagation characteristics assuming crystal lengths and pulse characteristics such that the optical pulse shape would distort significantly. Although (4.1) and (3.1) were solved numerically, the envelope changes are more transparent when considered in terms of the internal energy associated with the optical field, $\rho = \mathcal{E}\,(1 + \delta\epsilon)\mathcal{E}^*/8\pi$. This energy profile, which is independent of the phase of $\mathcal{E}$, distorts both through a nonlinear change in velocity, $-c\,\frac{\delta\epsilon}{2\epsilon_o}$ as well as through a nonlinear energy conversion stimulated by the rectified field which is generated. The latter is given by $-\rho\,\frac{\partial(\delta\epsilon/2\epsilon_o)}{\partial t}$. The internal energy associated with the rectified field, $\frac{F^2\epsilon_s}{16\pi}$ obeys a simpler equation in which the only nonlinear term is that which describes the rectified field generation, $-\frac{\delta\epsilon}{2\epsilon_o}\left(\frac{\partial\rho}{\partial t}\right)$.

Before a significant amount of distortion takes place for $\epsilon_s = \epsilon_o$, F is quite accurately described by Eq. (4.4) in which the term proportional to z eventually dominates for crystals much longer than the optical pulse. The nonlinear velocity change is roughly zero in the center of the pulse.

Consequently, the stimulated energy conversion, which is proportional to the second time derivative of the intensity, dominates and is such that there is a decrease in the intensity. The peak decreases to about 1/e of its initial

value in a distance Z_d of about $2c\tau_p/\Delta$ where Δ is the maximum value of $\left[\frac{(4\pi\chi)\mathcal{E}\mathcal{E}^*}{\epsilon_o}\right]^{\frac{1}{2}}$ at $z = 0$, and τ_p is the pulse width. In order to conserve energy, this decrease must be associated with an increase in the rectified field energy as well as a growth on the wings of the optical pulse, which implies that the pulse disperses nonlinearly. Both the nonlinear velocity change and the stimulated gain on the wings are such that the internal energy ρ spreads symmetrically about the center of the pulse. This is illustrated in Fig. 4.2 for a pulse propagating through a crystal possessing an electro-optic coefficient equal to 5×10^{-5} esu. Z_d is then equal to 2 cm.

In the other extreme, for $\epsilon_s \gg \epsilon_o$ and a crystal length much greater than the pulse length, the theory of Kerr effect self-steepening is valid provided one assumes a negative intensity dependent index change. The leading edge of the pulse consequently steepens in a manner analogous to acoustic shock wave development. The steepening distance is given[11] by $0.194\ c\tau_e\sqrt{\epsilon_o}/\delta\epsilon_m$ where τ_e is the full 1/e width of the initial intensity profile and $\delta\epsilon_m$ is the maximum change in the dielectric constant across the pulse profile. $\delta\epsilon_m$ is about 10^{-4} in BSN for a quarter of a gigawatt/cm^2 pulse. If t_e is 20 psec, then this distance is of the order of 25 meters. A shorter and more intense pulse would decrease this distance significantly; however, for most cases of interest the distortion should be small and, hence, the modulation effects should dominate.

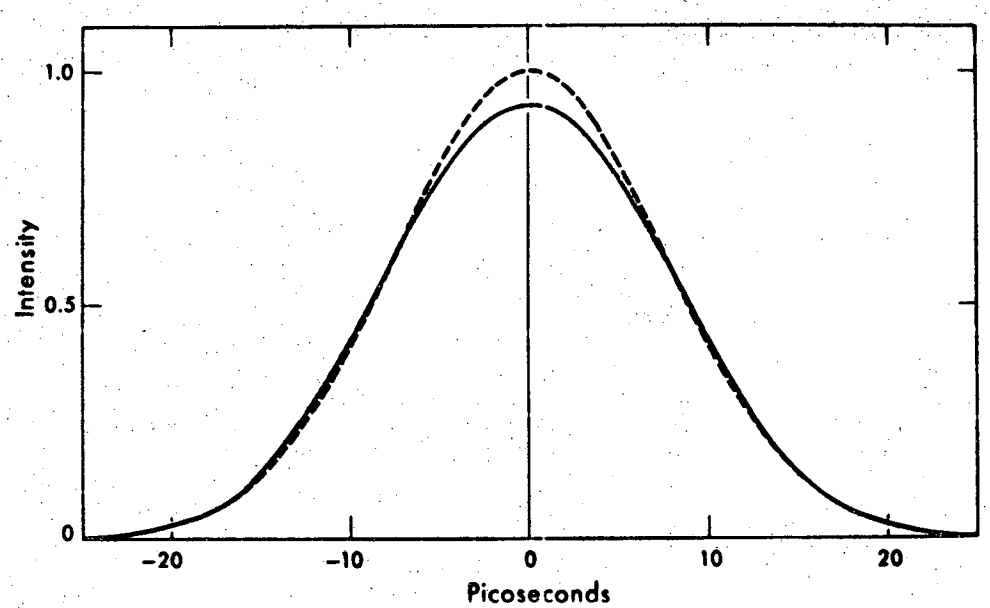

Fig. 4.2 Plot of the internal energy $(\epsilon_0 + 5\epsilon)\mathcal{E}\mathcal{E}^*/8\pi$ for a crystal of optical thickness 6 mm with an electro-optic coefficient of 5×10^{-5}. The initially Gaussian pulse has a full 1/e intensity width of 20 psec. and a peak intensity of .25 Gw/cm^2 (drawn dotted). The symmetrical spreading conforms with theoretical predictions.

V. Applications of Self-Phase-Modulation

Self-phase-modulation of optical pulses producing frequency broadening hundreds of wavenumbers in extent can easily dominate the initial phase profile across the pulse. Such self-phase-modulated spectra can be utilized to deduce information about the initial pulse shape. For the Kerr effect, the spectral width is roughly proportional to both the propagation distance and the size of the nonlinearity, and inversely proportional to the pulse duration. This has been established experimentally and has been employed to estimate the size of the nonlinearity associated with self-trapped filaments.[29] The filament duration could also be estimated since the frequency spacing between interference maxima close to the carrier frequency is the inverse of the pulse duration if both relaxation of the nonlinearity can be neglected and a large number of interference maxima are present. The self-phase-modulated spectrum may give more reliable pulse shape information than the presently used correlation techniques.

The large chirp resulting from self-phase-modulation also suggests the possibility of obtaining extremely short pulses with the use of dispersive delay techniques.[31-35] In particular, the linear frequency sweep introduced by a Kerr liquid near the peak of the pulse indicates that linearly dispersive optical delay lines can be utilized to delay the leading (lower frequency) portions of the pulse with respect to the lagging (higher frequency) portion.

We consider only "linear" nonattenuating dispersive delay devices (ones which cannot alter the frequency spectrum of the

pulse) and so the transfer function can be written as $\exp[-iQ(\omega)]$ where $Q(\omega)$ is real. One can then find the resultant complex electric field output by Fourier analyzing the pulse, applying the transfer function, and then Fourier reconstructing the pulse. For $\Omega \equiv \omega - \omega_o$ one finds for E_c, the complex compressed field [31, 34, 35]

$$E_c = \frac{e^{-i\omega_o t}}{2\pi} \int_{-\infty}^{\infty}\int dt' d\Omega \; a(t') \exp i[\delta\phi(t') + \Omega(t'-t) - Q(\Omega)] \qquad (5.1)$$

where $a(t')$ and $\delta\phi(t')$ are the input pulse electric field envelope and instantaneous phase shift respectively.

If we expand $Q(\Omega)$ in a power series (i.e. $Q(\Omega) = Q_o + Q_1\Omega + Q_2\Omega^2 + \ldots$), we see from Eq. (5.1) that Q_o (the overall phase) can be neglected. One also notices that the $Q_1\Omega$ term can be absorbed into the $\exp[i\Omega(t'-t)]$ by redefining t, and thus Q_1 corresponds to an equally uninteresting group delay. The $Q_2\Omega^2$ term is then the first important term in the series. We will assume that this term dominates the higher order terms, and we can effectively replace $Q(\Omega)$ in Eq. (5.1) by $Q_2\Omega^2$. One can then integrate over Ω to yield [33,35]

$$E_c = \frac{e^{-i[\frac{\pi}{4} + \omega_o t]}}{2\sqrt{\pi Q_2}} \; e^{\frac{it^2}{4Q_2}} \int_{-\infty}^{\infty} dt' a(t') \exp[i(\delta\phi(t') + \frac{t'^2}{4Q_2} - \frac{t't}{2Q_2})] \qquad (5.2)$$

A linearly chirped pulse, for example, has a quadratic time dependence of $\delta\phi$. Thus Q_2 of the dispersive delay line (or "compressor") can be adjusted so that the first two terms cancel in the exponent of Eq. (5.2), which implies that $\delta\phi = -\beta t'^2 = -\frac{t'^2}{4Q_2}$, or, equivalently, that $\beta^{-1} = 2Q_2$. If one further assumes that $a(t')$ is a Gaussian $[a(t') = a_o \exp(-(t')^2/2T_p^2)]$, then one can evaluate Eq. (5.2) to note that the intensity, $I(t)$ is given by:

$$I(t) \propto \exp\left[-t^2/(1/\beta T_p)^2\right] \tag{5.3}$$

which is a Gaussian pulse of duration $T_c \cong \frac{2}{\beta T_p}$. Since βT_p is of the order of the pulse bandwidth, one can see that the pulse has been compressed to near its uncertainty limit. Thus, one finds that an increase in the linear frequency sweep (and, hence, in the bandwidth) increases the possible compression efficiency.

In the case of an intense laser pulse propagating through a Kerr liquid, one finds that the resultant pulse does <u>not</u> exhibit a linear time dependence of instantaneous frequency shift. Thus, one cannot find a Q_2 which sets the expression $[\delta\phi(t') + t'^2/4Q_2]$ in Eq. (5.2) to zero over the entire pulse. The problem of compression of a self-phase-modulated pulse is most easily treated numerically.[34] To avoid unnecessary theoretical complications, we neglect envelope distortion (self-steepening) and assume that the pulse travels a distance which is much less than the self-focusing distance.

For a relaxation time short compared to the pulse duration Eq. (3.6) shows that the phase perturbation closely approximates the shape of the intensity profile. A symmetrical pulse thus develops an approximately constant positive chirp β_o near the intensity peak and the pulse envelope can be compressed by matching this chirp to the inverse of the delay per unit frequency of a delay line linearly dispersive in frequency. Since the effective bandwidth of the chirped pulse is of the order of $\beta_o T_p/2$ the minimum compressed pulse envelope width obtainable is of the order of $2/\beta_o T_p$. Compression is diminished by the

influence of relaxation which not only delays the maximum chirp, but also decreases the linear chirp in magnitude and extent. In the limit of T_p much shorter than the relaxation time, τ, Eq. (3.6) shows that the phase perturbation becomes monotonically increasing across the pulse since $\delta\phi$ is then proportional to the time-integrated intensity. The chirp is thus nonzero only on the wings of the pulse. Were such a pulse passed through the delay line, the most intense portion would remain uncompressed.

Figure (5.1) shows the instantaneous frequency shift which is found by numerical integration of Eq. (3.6) for an initially unmodulated Gaussian 22 Gw/cm^2 pulse of 5 picosecond full 1/e intensity duration propagating through 10 cm of CS_2 (relaxation time 2 picoseconds). The maximum index change is of the order of 1.5 down from the case of instantaneous relaxation. We estimate that neglecting envelope distortion due to the non-linearity and relaxation introduces about a 5% error over a propagation distance of 10 cm. The pulse can be compressed by matching the chirp near the intensity peak to the inverse of the delay per unit frequency of a delay line. The optimally compressed intensity profile is found by numerical evaluation of Eq. (5.2) for different values of Q_2. The resultant pulse envelope is shown in Fig. (5.2). The optimum value of Q_2 was numerically found to be $.65 \times 10^{-26}$ sec^2 for this particular case. The optimization point was found by increasing Q_2, which is proportional to the compressor setting, until the shortest pulse was found without substantial side lobes. These side lobes increased with further increase in Q_2 beyond the optimum value. For a compressor made of two

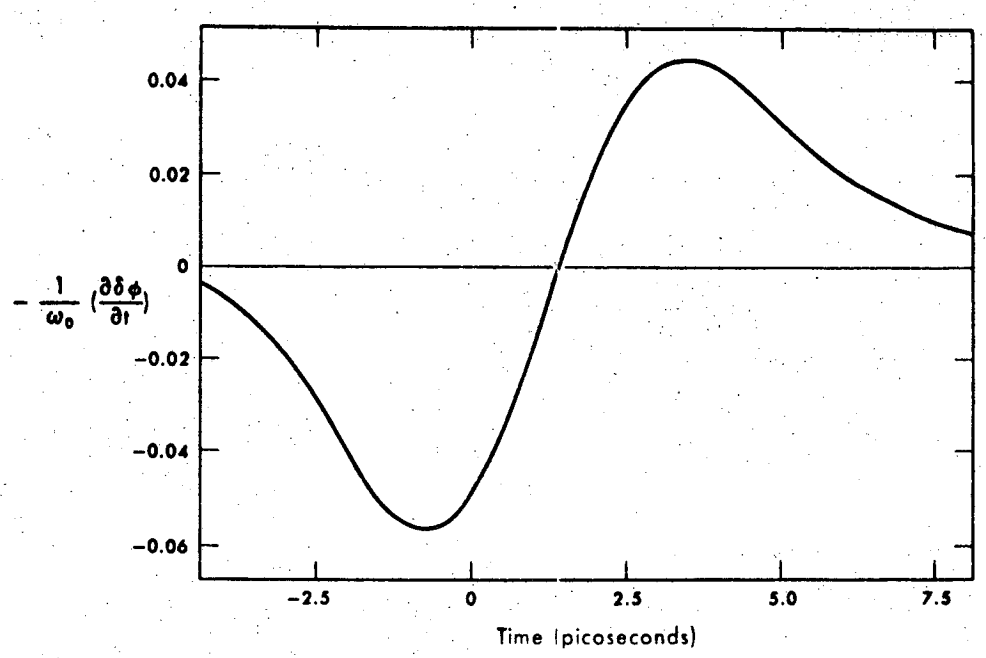

Fig. 5.1 Plot of the time derivative of the phase perturbation across an optical pulse for a 10 cm propagation distance in CS_2. the pulse has a peak intensity of 22 Gw/cm^2 and a full 1/e intensity width of 5 psec, and the relaxation time is 2 psec. The intensity peak occurs at 0.0 on the time axis. For a zero relaxation time the cross-over point would be at 0.0 and the maximum and minimum values would be 0.43 and -0.43, respectively.

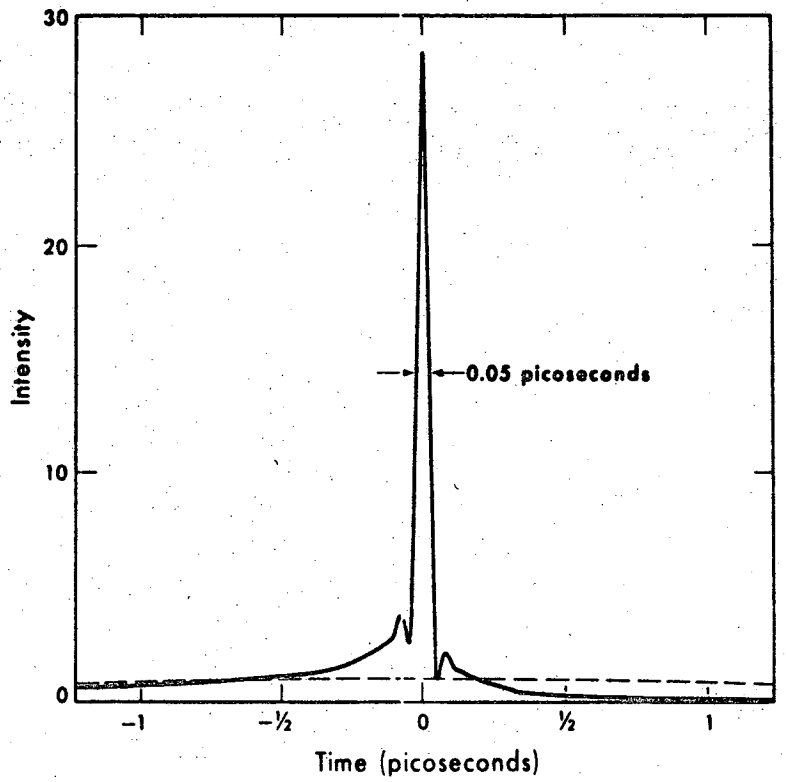

Fig. 5.2 The intensity profile of the optimally compressed pulse corresponding to the phase perturbation shown in Fig. 5.1. The initial Gaussian intensity is shown dotted. The intensities have been normalized to the initial peak intensity and the compressed pulse has been shifted so that the peaks coincide. The value of Q_2 which optimizes the compression corresponds to the slope of the curve in Fig. 5.1 evaluated at 0.31 psec.

parallel gratings having 300 lines per mm and oriented so that the angle of incidence of 60°, the grating separation to give the compression is 4 cm.

The full width at half-intensity of the optimally compressed pulse is 5×10^{-14}sec. These results are down by an order of magnitude from the estimates made neglecting relaxation and assuming a constant chirp over the pulse. The optimum value of Q_2 corresponds to the slope of the frequency shift at a point between the peak of the pulse and the point of maximum slope (and constancy of slope). Thus the maximum compressed pulse originates primarily from a region which simultaneously optimizes the intensity and constancy of slope. The case calculated here should be fairly realistic indicating that compression ratios of the order of 100 can be obtained using reasonable experimental conditions.

Although the calculations have been carried out specifically for unmodulated Neodymium pulses, intense mode-locked ruby pulses should serve equally well.

Pulse compression using the above technique has recently been achieved by Laubereau.[36]

REFERENCES

1. R. W. Hellwarth, Phys. Rev. 152, 156 (1966).

2. J. Frenkel, Kinetic Theory of Liquids (Dover, N.Y., 1945).

3. N. Bloembergen and P. Lallemand, Phys. Rev. Lett. 16, 81 (1966).

4. R. Y. Chiao, P. L. Kelley, and E. Garmire, Phys. Rev. Lett. 17, 1158 (1966).
   R. L. Carman, R. Y. Chiao, and P. L. Kelley, Phys. Rev. Lett. 17, 1281 (1966).

5. P. L. Kelley, Phys. Rev. Lett. 15, 1005 (1965).

6. R. Y. Chiao, E. Garmire, C. H. Townes, Phys. Rev. Lett. 13, 479 (1964).

7. P. Lallemand, Appl. Phys. Lett. 8, 276 (1966).
   K. Shimoda, Jap. J. Appl. Phys. 5, 615 (1966).

8. H. P. H. Grieneisen and C. A. Sacchi, Bull. Am Phys. Soc. 12, 686 (1967).
   R. G. Brewer, Phys. Rev. Lett. 19, 8 (1967).

9. F. Shimizu, Phys. Rev. Lett. 19, 1097 (1967).

10. A. C. Cheung, D. M. Rank, R. Y. Chiao, and C. H. Townes, Phys. Rev. Lett. 20, 786 (1968).

11. For a comprehensive discussion of small scale self-trapped filaments see:
    R. G. Brewer, J. R. Lifsitz, E. Garmire, R. Y. Chiao, C. H. Townes, Phys. Rev. 166, 326 (1968).

12. T. K. Gustafson, J. P. Taran, H. A. Haus, J. R. Lifsitz, and P. L. Kelley, Phys. Rev. 177, 1196

13. F. DeMartini, C. H. Townes, T. K. Gustafson and P. L. Kelley, Phys. Rev. 164, 312 (1967).

14. J. R. Lifsitz, and H. P. H. Grieneisen, Appl. Phys. Lett. 13, 245 (1968).

15. J. H. Marburger, W. G. Wagner, J. Quant, Elec. 3, 415 (1967).

16. J. A. Fleck, Jr. and P. L. Kelley, Appl. Phys. Lett. 15, 313 (1969).

17. N. M. Kroll, J. Appl. Phys. 36, 34 (1965).

18. N. M. Kroll and P. L. Kelley (to be published).

19. M. Bass, P. A. Franken, J. F. Ward, and G. Weinreich, Phys. Rev. Lett. 9, 446 (1962).

20. T. Y. Chang, N. VanTran, and C.K.N. Patel, Appl. Phys. Lett. 13, 357 (1968).
D. W. Faries, K. A. Gehring, P. L. Richards and Y. R. Shen, Phys. Rev. 180, 363 (1969).

21. A. J. DeMaria, W. H. Glenn,Jr., M.J. Brienza, and M.E. Mack, Proceeding of the IEEE 57, 2 (1969).

22. H. A. Smith and C. H. Townes, Polarisation, Matiere at Rayonnement, p. 467, edited by Societe Francaise de Physique, Presses Universitares de France (1969).

23. One Laplace transforms Eq. (4.1) in time and Fourier transforms in space, realizing that the latter is over the region $z \geq 0$. One then uses the fact that

$$\frac{1}{(2\pi)^2} \int_{-\infty}^{+\infty} dt \int_0^{\infty} dz \; e^{-iQz + i\Omega t} \mathcal{E}\mathcal{E}^* \quad \text{is equal}$$

to $\frac{1}{2}\left[(\delta(Q-\Omega/v_o)) - i\, P\left(\frac{1}{Q-\Omega/v_o}\right)\right]\mathcal{E}\mathcal{E}^*(\Omega)$ provided $\mathcal{E}\mathcal{E}^*$ is only a function of $(z-v_o t)$. The solution can also be obtained by taking a Fourier sum over the results of Ref. (24).

24. N. Bloembergen, Nonlinear Optics (W. A. Benjamin, Inc., New York, 1965) section 4-1 discusses parametric generation and boundary conditions for sinusoidal steady-state waves. Note in particular Eqs. (4-8), (4-9) and (4-10). See also N. Bloembergen and P. S. Pershan, Phys. Rev. 128, 193 (1962); Armstrong has also pointed out the time derivative obtained in Eq. (4.5). (private communication).

25. I. S. Rez, Usp. Fiz. Nauk 93, 633 (1967) [Soviet Physics Uspekhi 10, 759 (1968)].

26. P. V. Lenzo, E. G. Spencer, and A. A. Ballman, Appl. Phys. Lett. 11, 23 (1967).
G. Burns and A. W. Smith, IEEE J. Quantum Electron 4, 584 (1968).

27. For the Kerr effect the opposite is true. See Figure 5.1.

28. The fields reflected and transmitted are respectively:

$$F_r\left(t+\frac{z}{v_s}\right) = \frac{2\pi}{(\epsilon_s-\epsilon_o)}\left\{R_2 T_1' P\left(t+\frac{z}{v_s}-\frac{2L}{v_s}\right) - R_2' P\left(t+\frac{z}{v_s}-\frac{2L}{v_o}\right)\right\}$$

and

$$F_t\left(t-\frac{z}{v_s}\right) = \frac{2\pi}{(\epsilon_s-\epsilon_o)}\left\{T_2 T_1' P\left(t-\frac{z}{v_s}+\frac{2L}{v_s}\right) - T_2' P\left(t-\frac{z}{v_s}+\frac{2L}{v_o}\right)\right\}$$

28. (cont.) We have defined $T_2' = \frac{\sqrt{\epsilon_o}+\sqrt{\epsilon_s}}{\sqrt{\epsilon_s}+\sqrt{\epsilon_s}}$ and $R_2' = \frac{\sqrt{\epsilon_o} - \sqrt{\epsilon_s'}}{\sqrt{\epsilon_s} + \sqrt{\epsilon_s'}}$, the transmission and reflection coefficients pertaining to the forced response.

$$T_1 = \frac{2\sqrt{\epsilon_s'}}{\sqrt{\epsilon_s}+\sqrt{\epsilon_s'}},\quad R_1 = \frac{\sqrt{\epsilon_s'}-\sqrt{\epsilon_s}}{\sqrt{\epsilon_s}+\sqrt{\epsilon_s'}},\quad T_2 = \frac{2\sqrt{\epsilon_s}}{\sqrt{\epsilon_s}+\sqrt{\epsilon_s'}},\quad R_2 = -R_1$$

are the usual linear transmission and reflection coefficients at the input and output boundaries respectively. The reflected wave will subsequently be multiply reflected at $z = 0$ and $z = L$ with coefficient R_2. In the limit $\epsilon_s = \epsilon_o$, these become

$$F_r(t+\frac{z}{v_o}) = \frac{2\pi}{\sqrt{\epsilon_o}(\sqrt{\epsilon_o}+\sqrt{\epsilon_s'})}\left((\sqrt{\epsilon_o}-\sqrt{\epsilon_s'})\frac{\partial P}{\partial t}(t+\frac{z}{v_o}-\frac{2L}{v_o})\frac{z}{c}+\frac{2\sqrt{\epsilon_s'}}{\sqrt{\epsilon_s}+\sqrt{\epsilon_o'}}P(t+\frac{z}{v_o}-\frac{2L}{v_o})\right)$$

$$F_t(t-\frac{z}{v_o}) = \frac{2\pi}{\sqrt{\epsilon_o}(\sqrt{\epsilon_o}+\sqrt{\epsilon_s'})}\left(-2\sqrt{\epsilon_s'}\frac{\partial P}{\partial t}(t+\frac{z}{v_o}-\frac{2L}{v_o})\frac{z}{c} - \frac{\sqrt{\epsilon_s'}-\sqrt{\epsilon_o}}{\sqrt{\epsilon_o}+\sqrt{\epsilon_s'}}P(t+\frac{z}{v_o}-\frac{2L}{v_o})\right)$$

29. M. M. Denariez-Roberge and J. P. E. Taran, Appl. Phys. Lett. 14, (1969).

30. From Eq. (3.1) one can deduce a transport equation for ρ

$$\frac{\partial\rho}{\partial t} + \frac{\partial(\rho v)}{\partial z} + \frac{1}{2}\frac{\rho}{\epsilon_o}\frac{\partial\delta\epsilon}{\partial t} = 0$$ the proof of which is

given in Ref. (12). v is the nonlinear phase velocity given by $v = v_o(1 - 1/2\ \delta\epsilon/\epsilon_o)$. Since the rectified field obeys a linear equation, except for the source term, the energy equation for $\rho_d = \epsilon_s F^2/16\pi$ is much simpler:

$$\frac{\partial\rho_d}{\partial t} + v_s\frac{\partial\rho_d}{\partial z} + \frac{1}{2}\frac{\delta\epsilon}{\epsilon_o}\frac{\partial\rho}{\partial t} = 0$$

31. C. E. Cook, Proc. IRE 48, 310 (1960).

32. J. R. Klauder, A.C. Price, S. Darlington, and W.J. Albersheim, Bell System Tech. J. 39, 745 (1960).
F. Gires and P. Tournois, Compt. Rend. 258, 6112 (1964).
J. A. Giordmaine, M. A. Duguay, and J. W. Hansen, IEEE J. Quantum Electron. 4, 252 (1968).
E.B. Treacy, Appl. Phys. Lett. 14, 112 (1969).
M.A. Duguay and J.W. Hansen, Appl. Phys. Lett. 14, 14 (1969).

33. E. B. Treacy, Physics Letters 28A, 34 (1968).

34. R. A. Fisher, P. L. Kelley, and T.K. Gustafson, Appl. Phys. Lett. 14, 140 (1969).

35. E. B. Treacy, IEEE J. Quantum Electron. 5, 454 (1969).

36. A. Laubereau, Physics Letters 29A, 539 (1969).

LEGAL NOTICE

This report was prepared as an account of work sponsored by the United States Government. Neither the United States nor the United States Atomic Energy Commission, nor any of their employees, nor any of their contractors, subcontractors, or their employees, makes any warranty, express or implied, or assumes any legal liability or responsibility for the accuracy, completeness or usefulness of any information, apparatus, product or process disclosed, or represents that its use would not infringe privately owned rights.

TECHNICAL INFORMATION DIVISION
LAWRENCE RADIATION LABORATORY
UNIVERSITY OF CALIFORNIA
BERKELEY, CALIFORNIA 94720